Intraplate deformation of the Indian subcontinent

P. Banerjee,[1] R. Bürgmann,[2] B. Nagarajan,[3] and E. Apel[2]

Received 25 July 2008; revised 19 August 2008; accepted 21 August 2008; published 18 September 2008.

[1] While deformation at the Earth's surface primarily occurs along tectonic plate boundaries, major earthquakes have shaken regions deep within continental interiors. Three of the largest (M > 7.5) historic intraplate earthquakes occurred within the Indian subcontinent, suggesting the possibility of significant intraplate deformation. We consider surface velocities determined from new GPS data collected at 29 continuous GPS stations and 41 survey-mode GPS stations in India between 1995 and 2007 to find a north-south shortening rate of 0.3 ± 0.05 nanostrain yr^{-1}, which may be accommodated by 2 ± 1 mm/yr of more localized convergence across central India. Southward motions at 4–7 mm/yr of sites on the Shillong plateau in northeast India reflect rapid shortening and high earthquake hazard associated with active thrust faults bounding the plateau. The width and magnitude of the elastic strain accumulation field across the Himalaya varies little from ~76°–90° longitude, but the strain is more broadly distributed and convergence rates are higher along the eastern ~200 km of the range. **Citation:** Banerjee, P., R. Bürgmann, B. Nagarajan, and E. Apel (2008), Intraplate deformation of the Indian subcontinent, *Geophys. Res. Lett.*, *35*, L18301, doi:10.1029/2008GL035468.

1. Introduction

[2] The paradigm of plate tectonics is based on the premise of rigid, undeforming plates that interact along plate boundaries where deformation and earthquake faulting are localized; however, significant historic earthquakes have occurred deep in the interior of some plates. The observed occurrence of intraplate earthquakes [*Schulte and Mooney*, 2005] may reflect significant deformation or fragmentation of plate interiors. Alternatively, as stress in plate interiors may generally be near frictional failure levels [*Zoback et al.*, 2002], relatively modest and local perturbations of lithospheric stress or strength may be to blame for the occurrence of such events [*Grollimund and Zoback*, 2001; *Kenner and Segall*, 2000; *Pollitz et al.*, 2002]. Intraplate earthquakes are particularly challenging, as they strike regions that are often little prepared and much debate has been waged over how to assess earthquake hazards and probabilities in such regions [*Frankel*, 2004; *Newman et al.*, 1999].

[3] While most earthquakes of the Indian subcontinent occur along its northern boundary, where the Indian plate is thrust beneath southern Tibet along the Himalaya, a significant number of intraplate events have occurred (Figure 1a) [*Schulte and Mooney*, 2005]. The largest earthquakes in India away from plate boundaries occurred in the Gujarat region in western India, and near the Shillong Plateau in the northeast. The two largest events in the west were M ≈ 7.6 steep-reverse slip earthquakes that struck in 1819 and 2001 [*Bendick et al.*, 2001]. In northeast India, the great M ≈ 8 Assam earthquake of 1897 has been interpreted to have occurred on the steeply south-dipping Oldham fault rupturing to a depth of 35 km along the northern edge of the Shillong Plateau [*Bilham and England*, 2001]. A more active appearing structure, the Dauki fault bounds the plateau to the south. The Narmada-Son failed rift arm stretching across the Indian subcontinent has also been recognized as a zone of enhanced seismicity and deformation [*Rao*, 2000]. The steep dip of active fault structures is inherited from earlier extensional normal fault structures that formed in part during Precambrian rifting and/or were involved in the late Paleozoic breakup of Gondwana.

[4] A number of studies have focused on quantifying the magnitude of surface strain across continental interiors and determining the cause of such deformation using space geodetic measurements at mm/yr precision. For example, GPS measurements suggest that horizontal deformation across North America east of the Rocky Mountains amounts to ~ 1 mm yr^{-1} (≤1 nanostrain yr^{-1}), which is dominated by subtle deformation associated with Holocene glacial isostatic rebound [*Calais et al.*, 2006; *Sella et al.*, 2007]. Geodetic evidence for localized accelerated deformation in the epicentral region of three 1811–1812 M > 7 New Madrid earthquakes continues to be debated [*Calais et al.*, 2006; *Smalley et al.*, 2005]. Estimates of intraplate strain across India from early campaign-mode GPS data [*Paul et al.*, 2001] and historic seismic moment release [*Bird and Liu*, 2000; *Rao*, 2000] suggest deformation at 2–7 nanostrain yr^{-1} (north-south shortening) and 0.2–0.6 nanostrain yr^{-1}, respectively. Here we consider surface velocities determined from new GPS data collected at 29 continuous GPS stations and 41 survey-mode GPS stations in India between 1995 and 2007 to examine the distribution and magnitude of intraplate deformation across the Indian subcontinent.

2. GPS Data and Analysis

[5] The GPS data collected during the 1995–2007 period were processed using the GAMIT/GLOBK 10.21 software package [*Herring*, 2005; *King and Bock*, 2005] to produce time series of station coordinates and their rates. The survey-mode GPS sites were occupied annually, for ~5 days, and are mostly located within the Himalaya [*Banerjee and Bürgmann*, 2002]. The duration of the continuous GPS observations vary between 3–10 yrs. The loosely con-

[1] Wadia Institute of Himalayan Geology, Dehra Dun, India.
[2] Department of Earth and Planetary Science and Berkeley Seismological Laboratory, University of California, Berkeley, California, USA.
[3] Geodetic and Research Branch, Survey of India, Dehra Dun, India.

0094-8276/08/2008GL035468$05.00

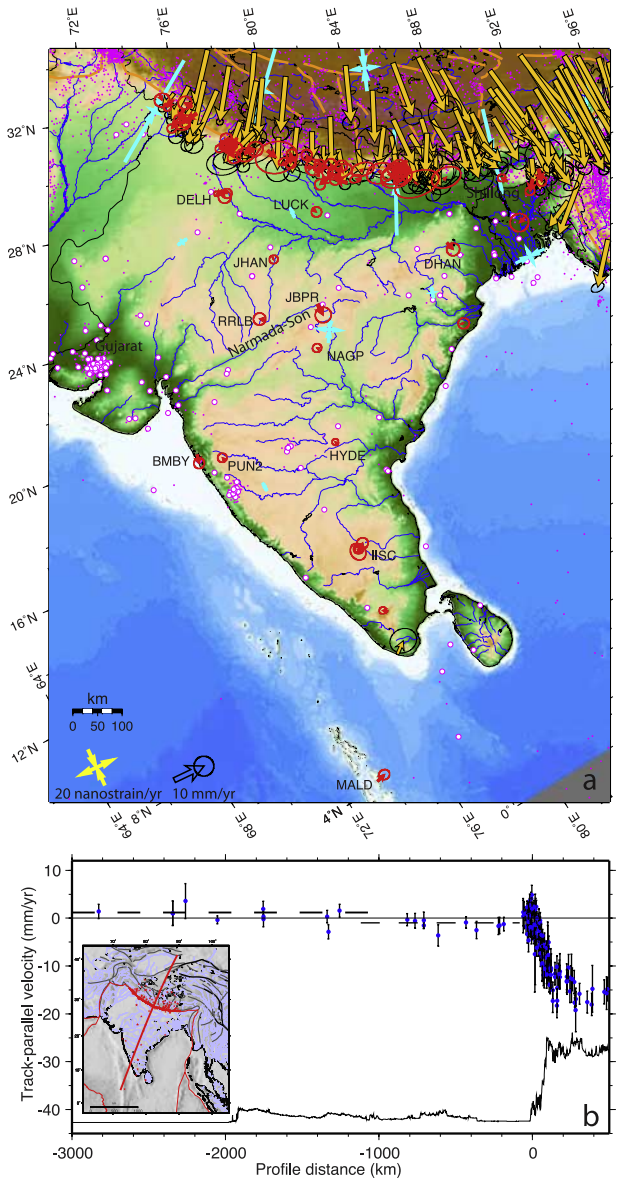

Figure 1. GPS velocities of India. (a) Map showing GPS velocities in India plate reference frame (tipped with 68% confidence ellipses) and derived principal strain axes and magnitudes using a distance-weighted strain interpolation approach [*Shen et al.*, 1996] (cyan crosses). Map is in oblique Mercator projection about India-Eurasia rotation pole (located at 21.8°E, 28.1°N, auxiliary material Data Set S2), where features and velocities parallel to the map border are in plate-convergence direction. Red arrows are GPS velocities of <4 mm/yr magnitude, orange arrows have larger rates with respect to India. Stations used to define the India reference frame are labeled with their station name (see auxiliary material). Magenta dots and circles indicate earthquakes from ANSS catalog (1935–2008) and intraplate catalog of *Schulte and Mooney* [2005], respectively. (b) North-south profile of GPS velocities across India (inset shows sites whose profile-parallel velocities are shown). Mean velocities of sites south of ~1000-km distance (near the Narmada Son lineament) and those in northern India (indicated by dashed lines) suggest convergence between southern and northern India of ~2 mm/yr.

strained solutions from our own processing were combined with loosely constrained solutions of ~125 globally distributed IGS station data available from the Scripps Orbital and Positioning Analysis Centre (SOPAC; http://garner.ucsd.edu). Using the GLOBK software [*Herring*, 2005], position estimates and velocity stabilization in ITRF00 were obtained using 45 and 63 core IGS tracking stations, respectively, resulting in 3 mm and 0.9 mm/yr RMS of the residuals. Coseismic corrections estimated from the position time series [*Banerjee et al.*, 2005] were applied to the Indian continuous GPS sites to remove the coseismic offsets from the 26th December, 2004 Sumatra-Andaman earthquake (Mw = 9.2). GPS velocities available from other published sources in the region [*Bettinelli et al.*, 2006; *Chen et al.*, 2000; *Gan et al.*, 2007; *Jade et al.*, 2007; *Kogan and Steblov*, 2008; *Sol et al.*, 2007; *Zhang et al.*, 2004] were combined with our own processed solutions using a 6-parameter Helmert transformation. An India reference frame is established by determining plate rotation parameters that minimize the velocities of 12 stations (10 continuous and 2 survey-mode GPS sites) well within the plate interior (see auxiliary material for details on sites used for the frame realization).[1] All velocities (in ITRF-2000 and India reference frames) are listed in auxiliary material Data Set S1 and Eurasian and Indian plate rotation parameters are listed in auxiliary material Data Set S2.

3. Results

[6] Figure 1a shows the GPS velocities in the India reference frame together with interpolated principal strain orientations and values computed across India and the Himalaya. Total intraplate strain calculated from all the low-velocity sites (<4 mm/yr with respect to stable India shown with red arrows in Figure 1a) spanning the nearly 3000 km distance between the Himalaya and the Maldives Islands is 0.3 ± 0.05 nanostrain yr^{-1} of north-south shortening across the Indian subcontinent. If we allow for this deformation to be localized in a deformation zone approximately aligned with the Narmada-Son lineament across central India, 2 ± 1 mm/yr of north-south convergence are indicated (dashed lines in Figure 1b indicate mean profile-parallel velocities of sites in southern and northern India). We formally test a scenario of independent plate motions north and south of the Narmada Son lineament using an F-test. Auxiliary material Figure S1 shows the residuals of the station velocities used in this analysis for the 1 and 2-plate realizations. The F-test shows that the 2-plate India model fits better at 89% confidence, below the typical 95%–99% values used in most plate circuit studies to confirm independent rigid plate motions [*Stein and Gordon*, 1984].

[7] From northwest India to eastern Nepal (~76° to 90°E), stations located in the foothills of the Himalaya in the hanging wall of the locked Main Frontal Thrust move insignificantly with respect to India. Thus, these stations lie outside of the zone of elastic strain accumulation, which is centered 80–140 km north of the surface trace of the thrust system [*Banerjee and Bürgmann*, 2002; *Larson et al.*, 1999]. India-Tibet convergence of ~17 mm/yr is distributed over a ~150-km-wide zone centered along the Greater Himalaya

[1] Auxiliary materials are available at ftp://ftp.agu.org/apend/gl/2008GL035468.

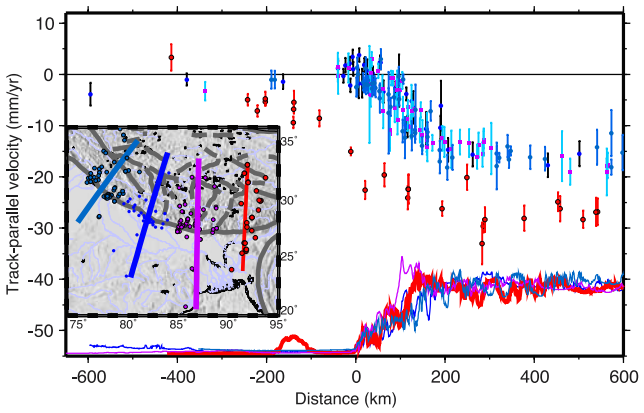

Figure 2. Deformation across northern India and the Himalaya. Swath profiles of Himalaya-normal GPS velocity components with respect to stable India. The inset shows the sites included for each of the four profiles identified by color. The lines at the bottom show the topography along each profile line drawn in the color of the associated velocity transect. Velocity gradients along the three western profiles track each other very closely. Along the eastern profile (red), convergence rates of southeastern Tibetan stations are ~10 mm/yr greater than those further west and sites on the Shillong plateau move southward at 4–7 mm/yr.

[*Bettinelli et al.*, 2006; *Feldl and Bilham*, 2006; *Larson et al.*, 1999] (Figure 2). The distribution and magnitude of contraction centered near the Greater Himalaya do not change appreciably along much of the Himalaya from northwestern India to eastern Nepal (Figure 2).

[8] The small motions of stations along the northwest Himalayan foothills as far west as 76° longitude suggest that western India is not deforming (Figure 1). However, we do not yet have velocity measurements across the northwest subcontinent to provide a direct estimate of deformation across the region. We also lack interseismic deformation measurements across the seismically active Gujarat region, because GPS-measured deformation in this area following the 2001 Bhuj earthquake has been dominated by post-earthquake transient motions [*Jade et al.*, 2002; *Reddy and Sunil*, 2007]. More GPS measurements in northwestern India and Pakistan are needed to fully resolve if widely distributed plate boundary deformation or plate fragmentation [*Stein et al.*, 2002] can be ruled out in this region.

[9] In contrast, contraction across the easternmost Himalaya is more rapid and more broadly distributed than along the remainder of the mountain chain. Arc-normal velocities along the eastern ~200-km extent of the Himalayan foothills do not approach stable Indian rates as they do along the remainder of the range, but range from 15–20 mm/yr (Figure 2, red profile), suggesting incomplete locking and/or active deformation well south of the Himalaya. The profile of GPS velocity components perpendicular to the Himalayan arc across the easternmost Himalaya also shows that the Himalaya-normal velocity of GPS sites in south Tibet are greater than those further west by nearly 10 mm/yr. The southward motions at 4–7 mm/yr of sites on the Shillong Plateau well to the south of the Himalayan range front indicate rapid contraction across its southern edge (Figure 3).

4. Discussion and Conclusions

[10] To evaluate fault slip rates and explore the first-order kinematics of the deformation across the Himalaya and Shillong Plateau, we develop a simple elastic model. The dislocation model includes elastic strain fields from two fault segments downdip of the locked Himalayan megathrust [*Larson et al.*, 1999], as well as contributions from thrust shear extending northward from deep below the N-dipping Dauki fault along the southern Shillong plateau edge (Figure 3). The model geometry and slip parameters are determined using non-linear inversion routines described by *Bürgmann et al.* [2002] following the approach described by *Larson et al.* [1999]. Strain accumulation from deep shear below the locked portion of active faults is represented by uniform-slip dislocations [*Okada*, 1985]. Importantly, the model suggests a greater slip rate of the Himalayan thrust under the Bhutan Himalaya than under the Nepal Himalaya, despite the 11 mm/yr loading rate we infer for the Shillong Plateau (see auxiliary material Table S1 for model parameters). This indicates that the transfer of contraction to the Shillong Plateau is balanced by increased net convergence rates between India and southern Tibet. This change in rate and distribution of deformation across the easternmost Himalaya may be related to the

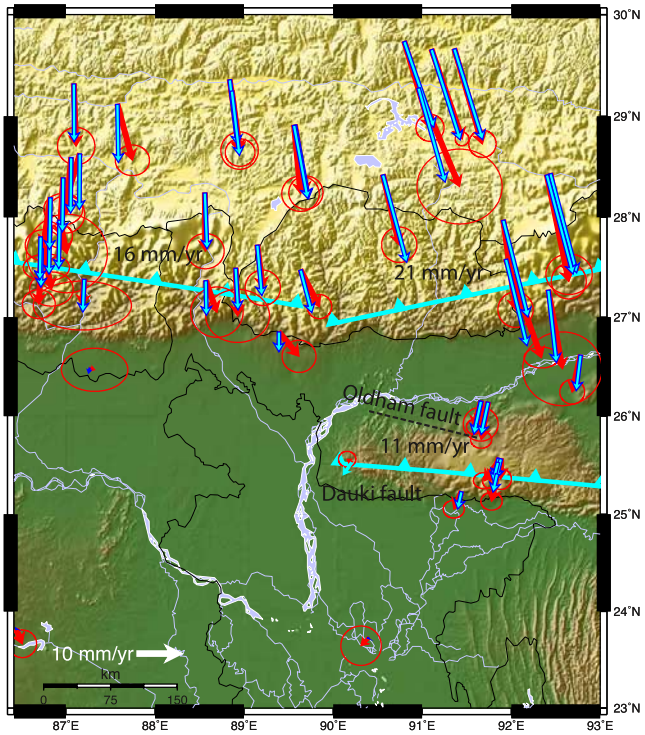

Figure 3. Northeast Himalaya and Shillong dislocation model. Close-up of NE India and Shillong plateau in Mercator projection with observed (red) and modeled (cyan) velocities. Updip, southern edges of three rectangular dislocations are labeled with optimal model slip rates. Model description and parameters are provided in auxiliary material Table S1.

geodynamics of the eastern Himalayan syntaxis and the rollback of the Indian slab beneath Burma [*Sol et al.*, 2007]. The rapid rate of contraction across the Shillong Plateau confirms the suspicion [*Bilham and England*, 2001] that the plateau-bounding Oldham and Dauki faults pose a great seismic threat to densely populated Bangladesh and northeast India. However, continued rapid convergence across Bhutan suggests that it may be premature to call for the impending demise of the eastern Himalaya [*Clark and Bilham*, 2008].

[11] Exhumation rates deduced from apatite and zircon (U-Th)/He and apatite fission track data suggest a convergence rate of 1–3 mm/yr across the plateau, since ~9 Ma [*Biswas et al.*, 2007; *Clark and Bilham*, 2008]. Our results indicate more than double that rate, suggesting geologically recent acceleration of fault slip rates along the Shillong plateau. The Late Cenozoic deformation involves reactivated passive-margin normal faults that developed during the Cretaceous breakup of India and Antarctica. A stretched and weakened lithosphere and preexisting faults exposed to plate boundary stresses allowed for the fragmentation of the Indian plate in its northeast corner. It is possible that the enhanced seismicity in the western Gujarat region is also made possible by a thinned and weakened lithosphere, possibly an enduring effect of heating from the plume head responsible for the Deccan flood basalts, which has been seismically imaged [*Kennett and Widiyantoro*, 1999]. However, there is no evidence for significant geologic shortening across this region and we lack geodetic constraints on pre-earthquake deformation rates.

[12] The GPS data indicate 2 ± 1 mm/yr of north-south shortening across the Indian subcontinent, which may be due to compressive plate boundary stress from the Himalayan continental collision zone. A model in which southern and northern India move independent of one another across the Narmada-Son line improves the fit to the data, but an F-test shows that such a two-plate model provides a statistically better fit at only 89% confidence. Tectonic stress generally appears to be near critical levels for frictional failure within plate interiors [*Zoback et al.*, 2002], and it is likely that small and local perturbations of lithospheric stress or strength are to blame for the occurrence and wide distribution of intraplate earthquakes in India.

[13] **Acknowledgments.** The work of P.B. and GPS data came from DST, Government of India funded projects, and from the National GPS Data Archive, Geodetic and Research Branch, Survey of India. This paper benefited from comments by an anonymous reviewer and M.G. Kogan. Berkeley Seismolab Contribution # 08-11.

References

Banerjee, P., and R. Bürgmann (2002), Convergence across the northwest Himalaya from GPS measurements, *Geophys. Res. Lett.*, *29*(13), 1652, doi:10.1029/2002GL015184.

Banerjee, P., F. Pollitz, and R. Bürgmann (2005), The size and duration of the Sumatra-Andaman earthquake from far-field static offsets, *Science*, *308*, 1769–1772.

Bendick, R., R. Bilham, E. Fielding, V. K. Gaur, S. E. Hough, G. Kier, M. N. Kulkarni, S. Martin, K. Mueller, and M. Mukul (2001), The 26 January 2001 "Republic Day" earthquake, India, *Seismol. Res. Lett.*, *72*, 328–335.

Bettinelli, P., J.-P. Avouac, M. Flouzat, F. Jouanne, L. Bollinger, P. Willis, and G. R. Chitrakar (2006), Plate motion of India and interseismic strain in the Nepal Himalaya from GPS and DORIS measurements, *J. Geod.*, *80*, 567–589.

Bilham, R., and P. England (2001), Plateau 'pop-up' in the great 1897 Assam earthquake, *Nature*, *410*, 806–809.

Bird, P., and Z. Liu (2000), Global finite-element model makes a small contribution to intraplate seismic hazard estimation, *Bull. Seismol. Soc. Am.*, *89*, 1642–1647.

Biswas, S., I. Coutand, D. Grujic, C. Hager, D. Stöckli, and B. Grasemann (2007), Exhumation and uplift of the Shillong plateau and its influence on the eastern Himalayas: New constraints from apatite and zircon (U-Th-[Sm])/He and apatite fission track analyses, *Tectonics*, *26*, TC6013, doi:10.1029/2007TC002125.

Bürgmann, R., M. E. Ayhan, E. J. Fielding, T. J. Wright, S. McClusky, B. Aktug, C. Demir, O. Lenk, and A. Türkezer (2002), Deformation during the 12 November 1999 Düzce, Turkey Earthquake, from GPS and InSAR Data, *Bull. Seismol. Soc. Am.*, *92*, 161–171.

Calais, E., J. Y. Han, C. DeMets, and J. M. Nocquer (2006), Deformation of the North American plate interior from a decade of continuous GPS measurements, *J. Geophys. Res.*, *111*, B06402, doi:10.1029/2005JB004253.

Chen, Z., B. C. Burchfiel, Y. Liu, R. W. King, L. H. Royden, W. Tang, E. Wang, J. Zhao, and X. Zhang (2000), Global Positioning System measurements from eastern Tibet and their implications for India/Eurasia intercontinental deformation, *J. Geophys. Res.*, *105*, 16,215–16,227.

Clark, M. K., and R. Bilham (2008), Miocene rise of the Shillong Plateau and the beginning of the end for the Eastern Himalaya, *Earth Planet. Sci. Lett.*, *269*, 336–350.

Feldl, N., and R. Bilham (2006), Great Himalayan earthquakes and the Tibetan plateau, *Nature*, *444*, 165–170.

Frankel, A. (2004), How can seismic hazard around the New Madrid Seismic Zone be similar to that in California?, *Seismol. Res. Lett.*, *75*, 575–586.

Gan, W. J., P. Zhang, Z. K. Shen, Z. Niu, M. Wang, Y. Wan, D. Zhou, and J. Cheng (2007), Present-day crustal motion with the Tibetan Plateau inferred from GPS measurements, *J. Geophys. Res.*, *112*, B08416, doi:10.1029/2005JB004120.

Grollimund, B., and M. D. Zoback (2001), Did deglaciation trigger New Madrid seismicity?, *Geology*, *29*, 175–178.

Herring, T. A. (2005), GLOBK, Global Kalman filter VLBI and GPS analysis program, version 10.2, report, Mass. Inst. of Technol., Cambridge, Mass.

Jade, S., M. Mukul, I. A. Parvez, M. B. Ananda, P. D. Kumar, and V. K. Gaur (2002), Estimates of coseismic displacement and post-seismic deformation using Global Positioning System geodesy for the Bhuj earthquake of 26 January 2001, *Curr. Sci.*, *82*, 748–752.

Jade, S., et al. (2007), Estimates of interseismic deformation in northeast India from GPS measurements, *Earth Planet. Sci. Lett.*, *263*, 221–234, doi:10.1016/j.epsl.2007.1008.1031.

Kenner, S., and P. Segall (2000), A mechanical model for intraplate earthquakes: Application to the New Madrid Seismic Zone, *Science*, *289*, 2329–2332.

Kennett, B. L. N., and S. Widiyantoro (1999), A low seismic wavespeed anomaly beneath northwestern India: A seismic signature of the Deccan Plume?, *Earth Planet. Sci. Lett.*, *165*, 145–155.

King, R. W., and Y. Bock (2005), Documentation for the GAMIT GPS Analysis software, release 10.2, report, Mass. Inst. of Technol., Cambridge, Mass.

Kogan, M., and G. Steblov (2008), Current global plate kinematics from GPS (1995–2007) with the plate-consistent reference frame, *J. Geophys. Res.*, *113*, B04416, doi:10.1029/2007JB005353.

Larson, K., R. Bürgmann, R. Bilham, and J. T. Freymueller (1999), Kinematics of the India-Eurasia collision zone from GPS measurements, *J. Geophys. Res.*, *104*, 1077–1093.

Newman, A. V., S. Stein, J. C. Weber, J. F. Engeln, A. Mao, and T. H. Dixon (1999), Slow deformation and lower seismic hazard at the New Madrid seismic zone, *Science*, *284*, 619–621.

Okada, Y. (1985), Surface deformation due to shear and tensile faults in a half-space, *Bull. Seismol. Soc. Am.*, *75*, 1135–1154.

Paul, J., et al. (2001), The motion and active deformation of India, *Geophys. Res. Lett.*, *28*, 647–651.

Pollitz, F., L. Kellogg, and R. Bürgmann (2002), Sinking mafic body in a reactivated lower crust: A mechanism for stress concentration in the New Madrid Seismic Zone, *Bull. Seismol. Soc. Am.*, *91*, 1882–1897.

Rao, B. R. (2000), Historical seismicity and deformation rates in the Indian Peninsular Shield, *J. Seismol.*, *4*, 247–258.

Reddy, C. D., and P. S. Sunil (2007), Post-seismic crustal deformation and strain rate in Bhuj region, western India, after the 2001 January 26 earthquake, *Geophys. J. Int.*, *172*, 593–606, doi:10.1111/j.1365-1246X.2007.03641.x.

Schulte, S. M., and W. D. Mooney (2005), An updated global earthquake catalogue for stable continental regions: Reassessing the correlation with ancient rifts, *J. Geophys. Int.*, *161*, 707–721.

Sella, G. F., S. Stein, T. H. Dixon, M. Craymer, T. S. James, S. Mazzotti, and R. Dokka (2007), Observation of glacial isostatic adjustment in stable North America with GPS, *Geophys. Res. Lett.*, *34*, L02306, doi:10.1029/2006GL027081.

Shen, Z. K., D. Jackson, and B. Ge (1996), Crustal deformation across and beyond the Los Angeles basin, *J. Geophys. Res.*, *101*, 27,957–27,980.

Smalley, R. F., M. A. Ellis, J. Paul, and R. B. Van Arnsdale (2005), Space geodetic evidence for rapid strain rates in the New Madrid seismic zone of central USA, *Nature*, *435*, 1088–1090.

Sol, S., et al. (2007), Geodynamics of the southeastern Tibetan plateau from seismic anisotropy and geodesy, *Geology*, *35*, 563–566.

Stein, S., and R. G. Gordon (1984), Statistical tests of additional plate boundaries from plate motion inversions, *Earth Planet. Sci. Lett.*, *69*, 401–412.

Stein, S., G. Sella, and E. Okal (2002), The January 26, 2001 Bhuj earthquake and the diffuse western boundary of the Indian plate, in *Plate Boundary Zones*, *Geodyn. Ser.*, vol. 30, edited by S. Stein, and J. Freymueller, pp. 243–254, AGU, Washington, D. C.

Zhang, P., et al. (2004), Continuous deformation of the Tibetan Plateau from GPS, *Geology*, *32*, 809–812.

Zoback, M. D., J. Townend, and B. Grollimund (2002), Steady-state failure equilibrium and deformation of intraplate lithosphere, *Int. Geol. Rev.*, *44*, 383–401.

E. Apel and R. Bürgmann, Department of Earth and Planetary Science and Berkeley Seismological Laboratory, University of California, Berkeley, 4767 McCone Hall, Berkeley, CA 94720, USA. (burgmann@seismo.berkeley.edu)

P. Banerjee, Wadia Institute of Himalayan Geology, Dehra Dun 248001, India.

B. Nagarajan, Geodetic and Research Branch, Survey of India, Dehra Dun 248001, India.

Supplementary Information

The GPS data were processed using the GAMIT/GLOBK software package [*Herring*, 2005; *King and Bock*, 2005] to produce time series of station coordinates and their rates in the ITRF-2000 reference frame. The GPS data collected during the 1995-2007 period, from 29 Continuous GPS (CGPS) stations and 106 Survey-mode GPS (SGPS) stations in India, were processed using the GAMIT/GLOBK 10.21 suit of software [*King and Bock*, 2005]. The SGPS sites were occupied annually, for ~5 days, and are mostly located within the Himalaya. The duration of the CGPS sites vary between 3-10 yrs. Much of the CGPS data were provided by the Survey Of India GPS Data Archive, while the SGPS measurements and data from 10 CGPS sites were collected by PB under various Dept. of Science & Technology, Govt. of India funded projects. IISC and HYDE are IGS sites. Additional 6-8 IGS station data from the surrounding regions were included while processing the data on a daily basis producing loosely constrained station coordinates and satellite orbits. These were further combined with loosely constrained solutions of ~125 globally distributed IGS station data available from the Scripps Orbital and Positioning Analysis Centre (SOPAC; http:garner.ucsd.edu). Using the GLOBK software [*Herring*, 2005], position estimates and velocity stabilization in ITRF00 were achieved using 45 and 63 core IGS tracking stations respectively, resulting in 3 mm and 0.9 mm/yr RMS of the residuals. Static correction of 2-18 mm were applied to the Indian CGPS sites to remove the coseismic offsets of the 26th December, 2004 Sumatra-Andaman earthquake (Mw=9.2) which were estimated from the time-series [*Banerjee, et al.*, 2005] of the station coordinates.

GPS velocities in our study region and for regional IGS GPS sites are listed in **Table S1**. Eurasian plate motion parameters (EURA) for the velocity field were realized by minimizing velocities of ten IGS stations (VILL, YAKT, IRKT, KSTU, ARTU, METS, POTS, WTZR, NYAL, and BRUS) representing the stable Eurasian plate. The Indian reference frame (INDI) was realized using 12 (10- CGPS, 2- SGPS) station data (DHAN, LUCK, JBPR, NAGP, JHAN, HYDE, IISC, RRLB, DELH, PUN2, MALD and BMBY). The velocities to define the reference frame were chosen so that the sites are away from known plate boundary zones and residuals are minimized. Even though motions of SGPS sites in the Himalayan foothills show insignificant motions with respect to stable India, none of these sites were included in the definition of Indian motion.. The wide distribution and small magnitude of the residual motions with respect to India shows that the motion of India is tightly constrained by this solution and not affected by the

choice of stations used for the reference frame. Uncertainties in Euler pole parameters computed for India and India-Eurasia plate motions computed here are much less compared to previously published results, where only two to four CGPS sites were used to establish Indian plate motion. Euler poles estimated for India and Eurasia plates (Table S2) have corresponding uncertainties of ~0.8 mm/yr and ~0.3 mm/yr in site motions, respectively. **Figure S1a** shows the magnitude of residuals of the plate-interior stations. We also examine a scenario of separate motion of Indian sub-plates north and south of the Narmada-Son lineament whose residuals are shown in **Figure S1b.**

GPS velocities available from other published sources [*Bettinelli, et al.*, 2006; *Chen, et al.*, 2000; *Gan, et al.*, 2007; *Jade, et al.*, 2007; *Kogan and Steblov*, 2007; *Sol, et al.*, 2007; *Wang, et al.*, 2001; *Zhang, et al.*, 2004], covering the entire Himalayan arc and the adjacent part of Tibet, were combined with our own processed solutions using the GLOBK utility programs [*Herring*, 2005]. Six component transformation parameters between two sets of horizontal velocities were computed using a group of common sites. Transformations between ITRF00, EURA and INDI reference frames were realized using the estimated EURA and INDI plate parameters (three Cartesian components of angular velocities:Wx,Wy,Wz) listed in **Table S2**. Typical RMS of the residuals of the transformed velocities is ~0.5 mm/yr.

Table S3 provides the geometry and slip rates for the deep dislocation model shown in Figure 1B. Calculations of elastic surface displacements due to uniform slip on rectangular dislocations at depth rely on the Okada [1985] algorithm.

References:

Banerjee, P., F. Pollitz, and R. Bürgmann (2005), The size and duration of the Sumatra-Andaman earthquake from far-field static offsets, *Science*, *308*, 1769-1772.

Bettinelli, P., J.-P. Avouac, M. Flouzat, F. Jouanne, L. Bollinger, P. Willis, and G. R. Chitrakar (2006), Plate motion of India and interseismic strain in the Nepal Himalaya from GPS and DORIS measurements, *J.Geod.* , *80*, 567-589.

Bürgmann, R., M. E. Ayhan, E. J. Fielding, T. J. Wright, S. McClusky, B. Aktug, C. Demir, O. Lenk, and A. Türkezer (2002), Deformation during the 12 November 1999 Düzce, Turkey Earthquake, from GPS and InSAR Data, *Bull. Seism. Soc. Am.*, *92*, 161-171.

Chen, Z., B. C. Burchfiel, Y. Liu, R. W. King, L. H. Royden, W. Tang, E. Wang, J. Zhao, and X. Zhang (2000), Global Positioning System measurements from eastern Tibet and their

implications for India/Eurasia intercontinental deformation, *Journal of Geophysical Research*, *105*, 16215-16227.

Gan, W. J., P. Zhang, Z. K. Shen, Z. Niu, M. Wang, Y. Wan, D. Zhou, and J. Cheng (2007), Present-day crustal motion with the Tibetan Plateau inferred from GPS measurements, *J .Geophys. Res.*, *112*, doi:10.1029/2005JB004120.

Herring, T. A. (2005), GLOBK, Global Kalman filter VLBI and GPS analysis program, Version 10.2, *Mass. Instit. of Tech., Release 10.2*.

Jade, S., M. Mukul, A. K. Bhattacharya, M. S. M. Vijayan, S. Jaganathan, A. Kumar, R. P. Tiwari, A. Kumar, S. Kalita, S. C. Sahu, A. P. Krishna, S. S. Gupta, M. V. R. L. Murthy, and V. K. Gaur (2007), Estimates of interseismic deformation in Northeast India from GPS Measurements, *Earth and Planetary Science Letters*, doi: 10.1016/j.epsl.2007.1008.1031.

King, R. W., and Y. Bock (2005), Documentation for the GAMIT GPS Analysis software, *Mass. Instit. of Tech., Scripps Inst. Oceanogr., Release 10.2*.

Kogan, M., and G. Steblov (2007), Global plate kinematics from GPS in self-consistent reference frame, *EOS, Transactions American Geophysical Union*, *88*, Fall Meet. Suppl., Abstract G13C-07.

Larson, K., R. Bürgmann, R. Bilham, and J. T. Freymueller (1999), Kinematics of the India-Eurasia collision zone from GPS measurements, *Journal of Geophysical Research*, *104*, 1077-1093.

Okada, Y. (1985), Surface deformation due to shear and tensile faults in a half-space, *Bull. Seism. Soc. Am.*, *75*, 1135-1154.

Sol, S., A. Meltzer, R. Bürgmann, R. D. van der Hilst, R. King, Z. Chen, P. Koons, E. Lev, Y. P. Liu, B. P. K. Zeitler, X. Zhang, J. Zhang, and B. Zurek (2007), Geodynamics of the southeastern Tibetan plateau from seismic anisotropy and geodesy, *Geology*, *35*, 563-566.

Wang, Q., P. Zhang, J. T. Freymueller, R. Bilham, K. M. Larson, X. Lai, X. You, Z. Niu, J. Wu, Y. Li, J. Liu, Z. Yang, and Q. Chen (2001), Present-day crustal deformation in China constrained by Global Positioning System measurements, *Science*, *294*, 574-577.

Zhang, P., Z. K. Shen, M. Wang, W. Gan, R. Bürgmann, P. Molnar, Z. Niu, J. Sun, Q. Wang, J. Wu, H. Sun, and X. You (2004), Continuous Deformation of the Tibetan Plateau from GPS, *Geology*, *32*, 809-812.

Table S1: GPS-measured velocities in both ITRF-2000 and in India reference frame, including regional IGS stations

Site_Name*	*Lat* °N	*Long* °E	ITRF00 (mm/yr)					India (mm/yr)					Duration	Months
			Vn	Ve	Sn	Se	ρ	Vn	Ve	Sn	Se	ρ		
MALD_GPa	4.189	73.526	32.75	46.29	0.99	1.11	0.002	0.62	2.73	0.99	1.11	0.002	2002.1-2006.5	37
TIRO_GPa	8.423	76.969	35.42	46.38	2.37	2.77	-0.009	2.80	3.56	2.37	2.77	-0.009	2004.1-2005.1	9
KODI_GPn	10.230	77.470	33.38	41.22	0.52	0.56	0.006	0.70	-1.20	0.52	0.56	0.006		
CARI_GPa	11.613	92.719	28.22	34.47	1.25	1.78	-0.030	-5.14	-9.35	1.25	1.78	-0.030	1996.1-1999.8	8
IISC_GPa	13.021	77.570	33.51	41.14	0.61	0.64	-0.004	0.82	-0.53	0.61	0.64	-0.004	1996.1-2007.4	66
BAN2_GPa	13.034	77.512	34.46	43.65	1.10	1.15	0.001	1.78	1.99	1.10	1.15	0.001	2003.6-2007.4	36
HYDE_GPa	17.417	78.551	34.07	40.01	0.64	0.65	-0.003	1.27	-0.43	0.64	0.65	-0.003	1997.1-2007.4	61
PUN2_GPa	18.558	73.882	33.21	38.80	0.91	0.93	0.000	1.04	-0.41	0.91	0.93	0.000	2002.1-2007.0	43
BMBY_GPa	19.133	72.916	29.48	38.47	1.04	1.07	0.002	-2.53	-0.34	1.04	1.07	0.002	2002.2-2006.2	35
BHBN_GPa	20.263	85.792	33.38	41.30	1.09	1.13	0.000	0.05	0.43	1.09	1.13	0.000	2002.1-2005.8	36
NAGP_GPa	21.394	79.276	33.39	38.75	0.85	0.93	0.002	0.52	-0.41	0.85	0.93	0.002	2001.1-2007.4	5
JBPR_GPa	23.129	79.876	29.42	39.19	1.54	1.62	0.001	-3.51	0.57	1.54	1.62	0.001	2002.7-2004.7	21
RRLB_GPa	23.209	77.447	33.46	36.69	1.21	1.24	0.001	0.80	-1.36	1.21	1.24	0.001	2003.7-2006.7	34
AIWL_GPn	23.720	92.730	28.25	33.21	0.54	0.56	0.039	-5.10	-8.16	0.54	0.56	0.039		
DHAK_GPS	23.727	90.401	37.65	42.48	1.81	1.86	-0.001	4.25	1.65	1.81	1.86	-0.001		
DHAN_GPa	23.815	86.444	31.00	40.97	1.27	1.31	0.001	-2.35	1.09	1.27	1.31	0.001	2003.2-2005.8	29
H218_ZHr	24.013	97.856	-7.94	22.03	1.28	1.72	-0.020	-40.99	-20.46	1.28	1.72	-0.020		
H213_ZHr	24.712	97.943	-12.66	21.27	1.19	1.53	-0.018	-45.70	-21.08	1.19	1.53	-0.018		
IMPH_GPn	24.740	93.930	18.30	28.17	0.63	0.73	0.027	-15.00	-13.20	0.63	0.73	0.027		
NOPE_GPn	25.230	91.440	30.43	38.75	0.69	0.88	0.015	-2.95	-1.87	0.69	0.88	0.015		
MUNN_GPn	25.410	91.840	28.25	39.27	0.69	0.88	0.015	-5.12	-1.39	0.69	0.88	0.015		
JHAN_GPa	25.452	78.608	32.45	37.41	0.84	0.88	0.002	-0.34	0.04	0.84	0.88	0.002	2001.1-2007.4	5
TURA_GPn	25.530	90.210	35.07	39.00	0.59	0.69	0.017	1.67	-1.22	0.59	0.69	0.017		
SHLN_GPa	25.566	91.885	29.69	40.34	0.96	0.98	0.000	-3.68	-0.28	0.96	0.98	0.000	2002.2-2007.0	50
CSOS_GPn	25.570	91.860	29.25	38.47	0.52	0.54	0.030	-4.12	-2.15	0.52	0.54	0.030		
GHTY_GPn	26.140	91.740	25.98	38.67	0.69	0.88	0.013	-7.39	-1.74	0.69	0.88	0.013		
GHTU_GPn	26.150	91.660	28.59	38.56	0.52	0.54	0.028	-4.78	-1.82	0.52	0.54	0.028		
GAUH_GPa	26.153	91.661	29.04	40.08	1.56	1.60	-0.001	-4.33	-0.30	1.56	1.60	-0.001	2003.1-2005.0	24
LUMA_GPa	26.220	94.475	24.61	39.13	1.35	1.41	-0.003	-8.66	-1.95	1.35	1.41	-0.003	2004.3-2007.0	24
BIRA_ZHr	26.484	87.264	33.95	40.75	1.74	2.95	0.053	0.58	1.61	1.74	2.95	0.053		
TZPR_GPa	26.618	92.780	25.93	38.38	1.13	1.14	0.000	-7.41	-2.14	1.13	1.14	0.000	2003.5-2007.0	38
JANK_ZHr	26.711	85.924	33.11	39.63	2.31	4.56	0.067	-0.22	0.92	2.31	4.56	0.067		
RBIT_GPa	26.849	89.392	28.82	43.84	1.48	1.56	0.002	-4.58	4.28	1.48	1.56	0.002	2003.8-2006.0	26
LUCK_GPa	26.891	80.943	32.06	38.11	1.01	1.04	0.000	-0.96	0.77	1.01	1.04	0.000	2001.7-2005.9	45
SIMA_ZHr	27.163	84.982	34.50	38.96	1.47	2.38	0.024	1.21	0.67	1.47	2.38	0.024		
NIJ0_GPk	27.183	85.187	36.89	38.20	1.01	1.09	-0.001	3.59	-0.13	1.01	1.09	-0.001		
BOMD_GPa	27.270	92.415	16.56	43.17	3.39	3.64	-0.002	-16.79	2.95	3.39	3.64	-0.002	2004.1-2004.7	7
HET0_GPk	27.316	85.008	34.58	37.40	1.01	1.09	-0.001	1.29	-0.83	1.01	1.09	-0.001		
GBSK_GPa	27.365	88.569	27.20	41.44	2.31	2.41	0.001	-6.19	2.28	2.31	2.41	0.001	2005.0-2006.0	13
KHAN_ZHr	27.380	87.206	28.36	38.78	2.05	4.47	0.074	-5.01	-0.01	2.05	4.47	0.074		
TIMP_GPa	27.472	89.635	26.05	43.40	1.11	1.13	0.000	-7.34	3.99	1.11	1.13	0.000	2003.1-2006.7	36
YADO_ZHr	27.489	88.906	23.60	40.05	2.26	2.83	-0.035	-9.79	0.84	2.26	2.83	-0.035		
KRN2_GPk	27.568	82.785	35.58	35.18	1.01	1.09	-0.001	2.42	-2.36	1.01	1.09	-0.001		
PKI0_GPk	27.575	85.398	33.19	39.58	1.01	1.09	-0.001	-0.12	1.34	1.01	1.09	-0.001		
BHAR_ZHr	27.678	84.430	32.53	38.60	1.77	2.70	0.042	-0.73	0.66	1.77	2.70	0.042		
NAGD_GPm	27.690	85.520	31.27	38.36	1.32	1.41	0.002	-2.04	0.14	1.32	1.41	0.002		
AIRP_ZHr	27.693	85.280	30.06	37.85	1.94	3.12	0.026	-3.24	-0.31	1.94	3.12	0.026		
NAGA_GPa	27.693	85.521	29.47	38.74	1.04	1.08	-0.002	-3.84	0.52	1.04	1.08	-0.002	1996.2-2000.5	19
J042_GPm	27.720	89.150	24.42	40.90	1.61	1.61	0.000	-8.97	1.71	1.61	1.61	0.000		
BAL0_GPk	27.745	85.794	30.92	36.77	1.01	1.09	-0.002	-2.40	-1.51	1.01	1.09	-0.002		
BMT0_GPk	27.786	82.540	35.66	36.38	1.01	1.09	-0.002	2.51	-1.00	1.01	1.09	-0.002		

Continued ...

Site_Name*	*Lat* °N	*Long* °E	ITRF00 (mm/yr)					India (mm/yr)					Duration	Months
			Vn	Ve	Sn	Se	ρ	Vn	Ve	Sn	Se	ρ		
KKNO_GPk	27.800	85.279	32.69	39.37	1.19	1.26	-0.001	-0.61	1.25	1.19	1.26	-0.001		
NAMC_ZHr	27.803	86.715	22.55	41.37	1.28	1.85	0.013	-10.80	2.87	1.28	1.85	0.013		
PHER_GPm	27.890	86.820	25.05	38.20	1.23	2.11	0.001	-8.31	-0.30	1.23	2.11	0.001		
CHPO_GPk	27.951	82.504	36.26	39.67	1.01	1.09	-0.002	3.12	2.37	1.01	1.09	-0.002		
SCOL_GPm	27.970	86.930	26.41	40.62	3.61	3.70	0.000	-6.95	2.12	3.61	3.70	0.000		
JO34_GPm	27.970	91.910	13.89	43.11	1.61	1.61	0.000	-19.47	3.26	1.61	1.61	0.000		
KUSO_GPk	28.010	82.095	32.04	34.36	1.01	0.99	-0.002	-1.07	-2.81	1.01	0.99	-0.002		
RAMO_GPk	28.015	85.222	27.08	39.36	1.01	1.08	-0.002	-6.22	1.35	1.01	1.08	-0.002		
AMPO_GPk	28.030	82.247	34.75	36.56	1.01	0.99	-0.002	1.62	-0.64	1.01	0.99	-0.002		
JO41_GPm	28.150	85.970	22.73	36.83	1.61	1.71	0.001	-10.60	-1.33	1.61	1.71	0.001		
SYAO_GPk	28.171	85.329	26.98	37.95	1.10	1.08	-0.001	-6.32	-0.03	1.10	1.08	-0.001		
RONG_ZHr	28.194	86.827	23.57	37.18	1.11	1.50	0.026	-9.79	-1.20	1.11	1.50	0.026		
BBPO_GPk	28.196	82.094	36.05	40.95	1.01	0.99	-0.002	2.94	3.86	1.01	0.99	-0.002		
JO29_GPm	28.240	88.560	20.91	39.45	1.61	1.71	0.000	-12.48	0.61	1.61	1.71	0.000		
MULO_GPk	28.249	82.347	35.45	37.45	1.01	0.99	-0.002	2.32	0.31	1.01	0.99	-0.002		
NYLM_ZHr	28.294	86.023	21.93	38.76	1.30	1.67	-0.055	-11.40	0.64	1.30	1.67	-0.055		
SPS2_GPk	28.407	81.691	34.83	38.14	1.00	0.99	-0.002	1.75	1.25	1.00	0.99	-0.002		
JO33_GPm	28.420	90.560	18.31	43.45	1.61	1.61	0.000	-15.08	4.13	1.61	1.61	0.000		
JO32_GPm	28.420	92.400	10.08	45.24	1.61	1.61	0.000	-23.27	5.41	1.61	1.61	0.000		
LOZ1_GPx	28.432	92.439	11.92	43.70	1.86	2.13	0.002	-21.43	3.86	1.86	2.13	0.002		
DELH_GPa	28.482	77.126	31.06	36.49	1.25	1.28	0.001	-1.56	0.88	1.25	1.28	0.001	2003.1-2005.8	26
DELO_GPa	28.544	77.172	31.43	37.08	0.96	1.00	0.000	-1.19	1.48	0.96	1.00	0.000	1997.8-2003.0	7
JO30_GPm	28.590	87.060	21.20	37.57	1.71	1.71	0.001	-12.16	-0.72	1.71	1.71	0.001		
LMK1_GPk	28.613	81.116	33.00	39.62	1.56	1.55	0.000	-0.03	2.98	1.56	1.55	0.000		
TING_ZHr	28.629	87.155	21.84	35.01	1.14	1.63	0.034	-11.52	-3.29	1.14	1.63	0.034		
GUCO_ZHr	28.783	86.340	20.28	42.47	3.39	3.98	0.018	-13.06	4.46	3.39	3.98	0.018		
GUTO_GPk	28.824	81.353	35.61	37.02	1.00	0.99	-0.002	2.56	0.41	1.00	0.99	-0.002		
JO39_GPm	28.910	89.560	18.63	40.79	1.61	1.71	0.000	-14.76	1.92	1.61	1.71	0.000		
JIAN_ZHr	28.914	89.573	19.10	41.70	1.24	1.39	-0.004	-14.29	2.83	1.24	1.39	-0.004		
JO40_GPm	28.960	85.440	20.44	37.51	1.71	1.71	0.001	-12.87	-0.18	1.71	1.71	0.001		
DLPO_GPk	28.983	82.818	23.08	36.92	1.09	1.08	-0.001	-10.08	-0.03	1.09	1.08	-0.001		
SHPO_GPk	29.012	80.636	35.28	37.11	1.00	0.99	-0.003	2.29	0.78	1.00	0.99	-0.003		
LAC1_GPx	29.082	93.082	7.82	45.84	0.93	1.12	0.011	-25.51	6.05	0.93	1.12	0.011		
LAZE_ZHr	29.118	87.577	21.70	42.03	1.11	1.39	-0.017	-11.67	3.80	1.11	1.39	-0.017		
MLX1_GPx	29.189	94.184	2.82	45.48	0.85	1.00	0.006	-30.46	5.41	0.85	1.00	0.006		
XIGA_ZHr	29.250	88.864	20.44	40.77	0.89	1.15	-0.004	-12.95	2.23	0.89	1.15	-0.004		
JMLO_GPk	29.277	82.191	28.15	35.80	1.00	0.98	-0.002	-4.97	-0.84	1.00	0.98	-0.002		
GGAR_GUr	29.278	90.959	12.14	48.73	3.32	3.85	0.010	-21.24	9.61	3.32	3.85	0.010		
JO38_GPm	29.320	87.090	19.91	38.95	1.71	1.71	0.000	-13.45	0.94	1.71	1.71	0.000		
DAD2_GPk	29.334	80.602	30.39	36.20	0.91	0.99	-0.003	-2.60	0.03	0.91	0.99	-0.003		
JO37_GPm	29.360	88.840	18.06	41.13	1.71	1.71	0.000	-15.33	2.64	1.71	1.71	0.000		
RAWU_GUr	29.391	96.868	-11.43	39.31	3.14	3.33	0.008	-44.55	-1.45	3.14	3.33	0.008		
SAGA_ZHr	29.441	85.214	21.62	33.34	1.11	1.36	-0.056	-11.68	-4.09	1.11	1.36	-0.056		
RWZ1_GPx	29.505	96.763	-9.65	42.75	0.81	0.88	-0.009	-42.77	2.06	0.81	0.88	-0.009		
SHBO_GPk	29.527	80.721	29.19	35.79	0.91	0.98	-0.003	-3.81	-0.33	0.91	0.98	-0.003		
PQX1_GPx	29.541	94.892	-1.70	45.10	0.83	0.99	-0.002	-34.94	4.95	0.83	0.99	-0.002		
SHOT_ZHr	29.591	85.741	18.61	40.69	3.41	3.98	0.014	-14.71	3.17	3.41	3.98	0.014		
LZX1_GPx	29.601	94.418	0.82	46.77	0.83	0.94	-0.005	-32.45	6.77	0.83	0.94	-0.005		
KTML_ZHr	29.638	79.620	30.39	38.47	3.08	4.12	-0.034	-2.50	2.71	3.08	4.12	-0.034		
LHAS_GPa	29.657	91.104	14.17	45.66	0.63	0.63	-0.002	-19.21	6.63	0.63	0.63	-0.002	1995.7-2007.0	105
DAGZ_ZHr	29.663	91.363	12.96	45.75	0.88	1.00	-0.016	-20.41	6.65	0.88	1.00	-0.016		
JO12_GPm	29.710	98.000	-13.27	43.36	1.71	1.71	0.000	-46.30	2.38	1.71	1.71	0.000		
ZUG1_GPx	29.727	97.778	-11.80	41.73	1.15	1.26	0.002	-44.84	0.82	1.15	1.26	0.002		
BALA_ZHr	29.736	90.798	14.87	45.10	0.87	1.06	-0.008	-18.51	6.19	0.87	1.06	-0.008		

Continued . . .

Site_Name*	*Lat* °N	*Long* °E	ITRF00 (mm/yr)					India (mm/yr)					Duration	Months
			Vn	Ve	Sn	Se	ρ	Vn	Ve	Sn	Se	ρ		
LAN2_GPa	29.848	78.680	32.66	38.08	1.45	1.55	-0.002	-0.14	2.69	1.45	1.55	-0.002	1998.6-2001.3	2
LANS_ZHr	29.848	78.680	30.10	36.25	2.13	2.91	-0.048	-2.70	0.86	2.13	2.91	-0.048		
ZMZ1_GPx	29.870	95.738	-4.82	47.12	0.93	1.25	-0.006	-38.01	6.84	0.93	1.25	-0.006		
GNGB_ZHr	29.881	93.237	2.05	55.50	3.37	3.93	0.009	-31.27	15.94	3.37	3.93	0.009		
GBD1_GPx	29.900	93.339	4.37	47.40	0.84	1.00	-0.001	-28.95	7.82	0.84	1.00	-0.001		
J022_GPm	29.940	93.150	4.91	47.80	1.71	1.71	0.000	-28.41	8.29	1.71	1.71	0.000		
J011_GPm	29.940	95.600	-5.35	46.44	1.71	1.71	0.000	-38.55	6.22	1.71	1.71	0.000		
BMZ1_GPb	30.055	96.886	-10.65	46.13	0.42	0.56	0.000	-43.76	5.58	0.42	0.56	0.000		
MUNS_GPa	30.060	80.240	23.43	33.19	2.31	2.35	0.001	-9.52	-2.54	2.31	2.35	0.001	2005.0-2006.0	13
RAJA_GPa	30.095	77.979	35.62	34.53	1.10	1.18	-0.007	2.90	-0.54	1.10	1.18	-0.007	1996.2-2001.3	6
TOM3_GKx	30.099	95.067	0.34	47.60	1.66	1.88	0.004	-32.89	7.59	1.66	1.88	0.004		
MOHA_GPa	30.147	77.868	29.09	36.34	1.12	1.31	0.012	-3.61	1.32	1.12	1.31	0.012	2001.3-2005.4	4
DOIW_GPa	30.191	78.187	32.54	34.01	0.89	0.92	0.005	-0.20	-1.07	0.89	0.92	0.005	1996.2-2002.2	7
QASI_GPa	30.276	77.630	31.66	34.01	0.76	0.81	0.000	-1.01	-0.87	0.76	0.81	0.000	1996.7-2005.4	7
WILD_GPa	30.285	77.974	30.80	34.71	0.71	0.77	0.011	-1.92	-0.27	0.71	0.77	0.011	1996.2-2005.4	9
J045_GPm	30.290	81.180	19.45	31.96	1.62	1.61	0.001	-13.59	-3.94	1.62	1.61	0.001		
GHOL_GPa	30.298	79.090	29.22	33.39	1.12	1.29	0.019	-3.62	-1.90	1.12	1.29	0.019	2001.4-2005.4	3
SABA_GPa	30.329	77.860	32.19	34.97	0.72	0.79	0.014	-0.51	0.05	0.72	0.79	0.014	1996.2-2005.4	8
WIHG_GPa	30.329	78.012	31.60	33.80	1.13	1.19	0.004	-1.12	-1.17	1.13	1.19	0.004	1996.2-2000.4	7
WIH2_GPa	30.329	78.014	31.75	33.44	0.73	0.74	0.000	-0.97	-1.53	0.73	0.74	0.000	1998.8-2007.0	82
POKH_GPa	30.329	79.194	29.92	31.23	1.10	1.16	0.006	-2.93	-4.08	1.10	1.16	0.006	2001.4-2005.4	3
DHAU_GPa	30.342	78.155	31.74	32.64	1.09	1.14	0.005	-1.00	-2.36	1.09	1.14	0.005	2001.3-2005.4	3
DHOU_GPa	30.342	78.155	31.61	34.55	1.12	1.16	0.006	-1.13	-0.45	1.12	1.16	0.006	1996.2-2000.5	5
J046_GPm	30.390	82.830	18.06	33.87	1.61	1.71	0.000	-15.10	-2.46	1.61	1.71	0.000		
CHMB_GPa	30.394	78.368	30.74	33.09	0.84	0.88	0.004	-2.02	-1.95	0.84	0.88	0.004	1998.6-2005.4	5
CHAM_ZHr	30.404	78.365	27.44	34.33	1.54	2.42	-0.100	-5.32	-0.70	1.54	2.42	-0.100		
BATA_GPa	30.452	78.115	29.30	35.57	1.28	1.38	0.039	-3.43	0.63	1.28	1.38	0.039	1996.2-2000.4	5
HATI_GPa	30.459	78.021	31.31	32.97	0.71	0.73	0.006	-1.41	-1.94	0.71	0.73	0.006	1996.2-2005.4	8
J021_GPm	30.480	91.110	13.81	46.17	1.71	1.81	0.000	-19.57	7.45	1.71	1.81	0.000		
AULI_ZHr	30.531	79.559	27.31	31.53	2.41	4.19	-0.064	-5.58	-3.79	2.41	4.19	-0.064		
BADR_GPa	30.743	79.493	21.42	27.90	1.11	1.26	0.017	-11.46	-7.30	1.11	1.26	0.017	2001.4-2005.4	3
J028_GPm	30.750	92.870	5.12	49.34	1.71	1.81	0.000	-28.21	10.20	1.71	1.81	0.000		
BHAT_GPa	30.806	78.617	27.02	31.20	1.11	1.14	0.004	-5.77	-3.71	1.11	1.14	0.004	2001.4-2005.4	3
SUKI_ZHr	30.997	78.676	22.16	28.87	1.53	2.38	-0.072	-10.63	-5.96	1.53	2.38	-0.072		
TCOQ_ZHr	31.019	85.139	17.60	34.13	3.40	3.93	0.019	-15.69	-2.61	3.40	3.93	0.019		
HARS_GPa	31.037	78.754	23.49	31.57	1.10	1.14	0.003	-9.31	-3.27	1.10	1.14	0.003	2001.4-2005.4	3
J026_GPm	31.130	88.690	14.66	42.86	1.81	1.81	0.000	-18.73	5.11	1.81	1.81	0.000		
J010_ZHr	31.162	97.169	-8.54	44.14	1.19	1.35	-0.005	-41.63	3.87	1.19	1.35	-0.005		
CAD1_GPr	31.164	97.122	-10.39	49.27	1.79	2.37	0.001	-43.48	9.01	1.79	2.37	0.001		
NAGQ_ZHr	31.469	92.036	9.07	49.00	1.23	1.38	-0.002	-24.29	10.38	1.23	1.38	-0.002		
BOHA_GPa	31.479	75.938	30.72	31.56	0.89	0.91	0.000	-1.74	-2.22	0.89	0.91	0.000	1998.9-2004.8	3
J020_GPm	31.510	92.070	6.96	49.49	1.71	1.81	0.000	-26.39	10.87	1.71	1.81	0.000		
UNAN_GPa	31.538	76.307	31.32	33.25	0.98	1.02	-0.001	-1.19	-0.61	0.98	1.02	-0.001	2001.7-2006.8	5
UNA0_ZHr	31.540	76.310	31.03	33.23	0.91	1.27	-0.055	-1.48	-0.63	0.91	1.27	-0.055		
REWL_GPa	31.634	76.815	31.53	30.91	0.76	0.77	0.000	-1.04	-3.05	0.76	0.77	0.000	1998.9-2006.8	6
SOXI_GUr	31.890	93.784	5.51	50.56	1.01	1.36	0.043	-27.78	11.56	1.01	1.36	0.043		
NYMA_GUr	31.891	87.766	15.29	41.49	3.15	3.32	0.006	-18.08	4.34	3.15	3.32	0.006		
JWLM_GPa	31.897	76.294	29.74	31.52	0.88	0.89	0.000	-2.76	-2.15	0.88	0.89	0.000	1998.9-2004.8	5
J019_ZHr	31.917	94.096	0.62	49.48	1.19	1.45	-0.005	-32.66	10.40	1.19	1.45	-0.005		
CHBG_GPa	31.919	76.673	34.23	31.85	1.29	1.36	0.001	1.68	-1.92	1.29	1.36	0.001	2001.7-2004.8	4
J036_GPm	31.930	86.440	15.88	39.36	1.71	1.81	0.000	-17.46	2.63	1.71	1.81	0.000		
J035_GPm	31.990	89.200	12.01	44.20	1.91	2.01	0.000	-21.38	6.65	1.91	2.01	0.000		
J025_GPm	32.010	91.110	8.23	46.54	1.81	2.01	0.000	-25.14	8.41	1.81	2.01	0.000		
KULU_GPa	32.067	77.108	24.32	26.58	0.89	0.91	0.000	-8.29	-7.25	0.89	0.91	0.000	1998.9-2004.7	4

Continued . . .

Site_Name*	*Lat* °N	*Long* °E	ITRF00 (mm/yr)					India (mm/yr)					Duration	Months
			Vn	Ve	Sn	Se	ρ	Vn	Ve	Sn	Se	ρ		
NADI_GPa	32.248	76.307	28.74	28.53	0.75	0.75	0.000	-3.76	-4.96	0.75	0.75	0.000	1998.9-2006.8	48
J018_GPm	32.250	91.670	6.39	47.82	1.81	2.10	0.000	-26.97	9.61	1.81	2.10	0.000		
Y226_GPm	32.270	96.500	-2.73	51.62	2.20	2.10	0.000	-35.87	11.93	2.20	2.10	0.000		
ANDU_ZHr	32.275	91.693	7.31	47.53	1.04	1.24	0.016	-26.05	9.32	1.04	1.24	0.016		
J043_ZHr	32.297	84.129	15.93	34.30	1.20	1.55	-0.030	-17.31	-1.56	1.20	1.55	-0.030		
NURP_GPa	32.304	75.881	30.65	31.34	0.77	0.78	0.000	-1.80	-2.00	0.77	0.78	0.000	1998.9-2006.8	6
KOT1_GPa	32.317	77.192	25.02	25.99	1.35	1.36	0.001	-7.60	-7.74	1.35	1.36	0.001	2003.8-2006.4	25
KOTH_GPa	32.317	77.192	18.18	26.69	1.13	1.19	0.001	-14.44	-7.04	1.13	1.19	0.001	1998.9-2002.7	3
KAZA_GPa	32.364	77.921	17.80	24.08	1.66	1.86	0.005	-14.91	-9.84	1.66	1.86	0.005	2004.7-2006.8	2
J044_GPm	32.380	81.190	16.36	30.59	1.62	1.61	-0.001	-16.67	-4.32	1.62	1.61	-0.001		
SQHE_GUr	32.427	79.800	15.46	28.10	3.15	3.33	0.005	-17.45	-6.36	3.15	3.33	0.005		
SHIQ_ZHr	32.509	80.098	15.74	30.23	1.39	1.73	-0.045	-17.20	-4.29	1.39	1.73	-0.045		
DALH_GPa	32.536	75.993	28.74	28.91	0.76	0.78	0.000	-3.72	-4.34	0.76	0.78	0.000	1998.9-2006.8	4
HIRA_GPa	32.565	75.363	30.75	33.37	1.37	1.54	-0.002	-1.62	0.33	1.37	1.54	-0.002	1998.9-2001.7	2
JIPA_GPa	32.634	77.175	18.95	23.87	1.39	1.44	-0.006	-13.66	-9.69	1.39	1.44	-0.006	1998.9-2001.7	2
UDAI_GPa	32.698	76.689	23.32	26.40	0.89	0.91	0.001	-9.23	-6.97	0.89	0.91	0.001	1998.9-2004.7	4
SRCH_GPa	32.798	77.425	17.27	27.24	1.67	1.80	0.004	-15.38	-6.31	1.67	1.80	0.004	2004.7-2006.8	3
BTX4_GPb	32.858	97.076	-2.58	49.38	0.59	0.65	-0.001	-35.67	9.72	0.59	0.65	-0.001		
J008_GPm	32.890	95.260	-2.11	52.29	2.00	2.00	0.000	-35.33	13.21	2.00	2.00	0.000		
TGLA_GUr	32.986	91.985	5.24	45.42	3.16	3.36	0.007	-28.11	7.40	3.16	3.36	0.007		
YUSH_GUr	32.997	96.988	-2.75	46.09	3.15	3.32	0.007	-35.85	6.50	3.15	3.32	0.007		
Y224_GPm	33.180	97.390	-5.46	51.26	1.70	1.70	0.000	-38.53	11.61	1.70	1.70	0.000		
NYOM_GPa	33.209	78.660	16.71	28.14	0.65	0.70	0.001	-16.08	-5.58	0.65	0.70	0.001	1995.7-2006.7	5
J049_GPm	33.560	79.940	15.51	30.03	1.62	1.61	-0.002	-17.41	-3.91	1.62	1.61	-0.002		
YANS_ZHr	33.649	92.056	5.34	47.80	1.06	1.26	-0.003	-28.01	10.03	1.06	1.26	-0.003		
DS39_GPm	33.900	97.270	-4.13	46.36	2.20	2.30	0.000	-37.21	7.01	2.20	2.30	0.000		
SHAK_GPa	33.972	77.808	16.84	26.67	1.12	1.25	0.004	-15.85	-6.38	1.12	1.25	0.004	2002.7-2006.7	3
SABU_GPa	34.130	77.613	18.80	26.76	0.65	0.68	0.003	-13.87	-6.15	0.65	0.68	0.003	1995.7-2006.7	7
TTHE_GPm	34.210	92.450	-0.83	48.64	1.71	1.91	0.000	-34.17	10.97	1.71	1.91	0.000		
TUOT_ZHr	34.214	92.447	1.13	49.09	1.42	1.94	0.058	-32.21	11.42	1.42	1.94	0.058		
ERDA_ZHr	34.631	92.854	2.39	46.63	2.11	2.70	0.030	-30.94	9.00	2.11	2.70	0.030		
KERN_GPa	34.642	73.970	-5.63	-9.55	2.99	3.17	-0.002	-37.79	-41.01	2.99	3.17	-0.002	2005.8-2006.6	9
PANA_GPa	34.710	77.576	19.73	27.37	1.32	1.45	0.004	-12.93	-5.21	1.32	1.45	0.004	2001.7-2004.7	4
PAN2_GPa	34.711	77.575	20.29	24.72	1.29	1.30	0.000	-12.37	-7.86	1.29	1.30	0.000	2003.8-2006.6	34
IGS stations used for velocity combination														
VILL_GPa	40.444	356.048	15.45	19.17	0.59	0.60	0.001	17.47	6.90	0.59	0.60	0.001	1995.7-2007.4	108
MAS1_GPa	27.764	344.367	16.05	15.77	0.59	0.60	0.003	24.77	-8.56	0.59	0.60	0.003	1995.7-2007.4	105
FORT_GPa	-3.877	321.574	10.82	-3.70	0.64	0.69	0.004	31.37	-49.72	0.64	0.69	0.004	1996.1-2006.2	50
KELY_GPa	66.987	309.055	10.91	-17.93	0.60	0.61	-0.002	36.61	-15.81	0.60	0.61	-0.002	1995.7-2007.4	107
STJO_GPa	47.595	307.322	11.01	-15.20	0.59	0.59	0.000	37.36	-30.11	0.59	0.59	0.000	1995.7-2007.4	108
GODE_GPa	39.022	283.173	2.89	-14.58	0.59	0.59	0.000	35.32	-44.14	0.59	0.59	0.000	1995.7-2007.4	106
ALGO_GPa	45.956	281.929	1.36	-16.12	0.59	0.59	0.000	33.94	-41.87	0.59	0.59	0.000	1995.7-2007.4	75
NLIB_GPa	41.772	268.425	-2.30	-15.36	0.59	0.59	0.000	31.06	-48.90	0.59	0.59	0.000	1995.7-2007.4	71
CHUR_GPa	58.759	265.911	-3.97	-17.68	0.61	0.62	0.001	29.30	-42.52	0.61	0.62	0.001	1996.2-2007.4	103
DUBO_GPa	50.259	264.134	-4.51	-16.94	0.66	0.66	0.000	28.70	-47.75	0.66	0.66	0.000	1998.1-2007.4	95
FLIN_GPa	54.726	258.022	-7.66	-17.20	0.76	0.77	0.001	25.02	-48.28	0.76	0.77	0.001	1996.6-2003.6	61
MDO1_GPa	30.681	255.985	-6.42	-12.55	0.58	0.59	0.001	26.04	-54.69	0.58	0.59	0.001	1995.7-2007.4	70
PIE1_GPa	34.302	251.881	-8.24	-13.21	0.59	0.59	0.001	23.57	-55.56	0.59	0.59	0.001	1995.7-2007.4	104
YELL_GPa	62.481	245.519	-11.24	-16.35	0.59	0.59	0.001	19.21	-48.90	0.59	0.59	0.001	1995.7-2007.4	70
DRAO_GPa	49.323	240.375	-10.81	-12.84	0.59	0.59	0.001	18.32	-54.08	0.59	0.59	0.001	1995.7-2007.4	74
TIDB_GPa	-35.399	148.980	54.90	18.00	0.61	0.63	0.007	37.94	-1.61	0.61	0.63	0.007	1996.6-2007.4	57
HOB2_GPa	-42.805	147.439	54.96	14.24	0.59	0.60	0.005	37.24	0.80	0.59	0.60	0.005	1995.7-2007.4	105
GUAM_GPa	13.589	144.868	2.12	-10.34	0.59	0.61	0.001	-16.87	-59.87	0.59	0.61	0.001	1995.7-2007.4	73
TIXI_GPa	71.634	128.866	-11.85	16.66	0.71	0.72	-0.002	-37.61	-17.39	0.71	0.72	-0.002	1998.9-2007.4	63

Continued . . .

Site_Name*	*Lat* °N	*Long* °E	ITRF00 (mm/yr)					India (mm/yr)					Duration	Months
			Vn	Ve	Sn	Se	ρ	Vn	Ve	Sn	Se	ρ		
KARR_GPa	-20.981	117.097	57.13	38.75	0.78	0.81	0.002	27.52	2.83	0.78	0.81	0.002	1998.2-2005.0	38
PERT_GPa	-31.802	115.885	57.06	39.00	0.59	0.60	0.001	27.15	9.05	0.59	0.60	0.001	1995.7-2007.4	104
CAS1_GPa	-66.283	110.520	-10.39	2.88	0.58	0.58	0.002	-41.50	-4.08	0.58	0.58	0.002	1995.7-2007.4	72
IRKT_GPa	52.219	104.316	-7.79	24.55	0.61	0.61	-0.002	-40.03	-9.39	0.61	0.61	-0.002	1996.1-2007.4	72
KSTU_GPa	55.993	92.794	-5.23	24.45	0.78	0.79	0.002	-38.52	-1.99	0.78	0.79	0.002	1997.8-2004.7	64
URUM_GPa	43.808	87.601	4.98	30.26	0.70	0.70	0.001	-28.37	-1.03	0.70	0.70	0.001	1998.9-2007.4	73
DAV1_GPa	-68.577	77.973	-6.07	-1.59	0.58	0.59	-0.002	-38.72	-24.03	0.58	0.59	-0.002	1995.7-2007.4	81
KERG_GPa	-49.351	70.256	-4.23	5.49	0.61	0.65	-0.018	-35.72	-31.78	0.61	0.65	-0.018	1996.1-2007.4	62
TRO1_GPa	69.663	18.940	14.01	14.03	0.67	0.67	0.001	2.93	28.01	0.67	0.67	0.001	1998.2-2007.4	96
MATE_GPa	40.649	16.704	17.71	23.98	0.59	0.60	0.000	7.85	10.97	0.59	0.60	0.000	1995.7-2007.4	105
GRAZ_GPa	47.067	15.493	14.25	21.95	0.59	0.60	0.000	5.07	15.09	0.59	0.60	0.000	1995.7-2007.4	90
POTS_GPa	52.379	13.066	14.02	19.13	0.59	0.59	0.000	6.20	17.61	0.59	0.59	0.000	1995.7-2007.4	109
WTZR_GPa	49.144	12.879	14.24	20.22	0.60	0.61	0.000	6.53	15.63	0.60	0.61	0.000	1996.1-2007.4	106
ONSA_GPa	57.395	11.926	13.61	16.97	0.59	0.59	0.000	6.44	20.39	0.59	0.59	0.000	1995.7-2007.4	106
NYAL_GPa	78.930	11.865	12.91	10.32	0.60	0.60	0.000	5.78	33.70	0.60	0.60	0.000	1995.7-2007.4	62
SEY1_GPa	-4.674	55.479	9.38	27.64	0.97	1.03	0.003	-18.31	-18.08	0.97	1.03	0.003	1996.1-2006.9	30
DGAR_GPa	-7.270	72.370	30.47	46.90	0.71	0.75	-0.003	-1.46	1.67	0.71	0.75	-0.003	1998.2-2007.4	52

*Data Source: Last letter of station suffix indicates the source of the GPS velocities used as follows:

a: from GPS analysis in this study.

b: Z. Chen et al., J. Geophys. Res. 105 doi:0148-0227/00/2000JB900092 (2000).

k: P. Bettinelli et al.,J.Geod. DOI:10.1007/s00190-006-0030-3 (2006)

m: W. Gan et al., J. Geophys. Res., Vol.112,B08416,doi:10.1029/2005JB004120 (2007)

n: S. Jade et al.,Earth Planet. Sci. Lett., doi:10.1016/j.epsl.2007.08.031 (2007)

r: P. Zhang et al., Geology, 32 doi:10.1130/G20554.1 (2004)

R: Q. Wang et al., Science, 294, 574-577 (2001)

S: M. Kogan and Steblov, EOS Trans,AGU88, Fall Meet. Suppl. (2007)

x: S. Sol et al., Geology, 35, doi:10.1130/G23408A.1 (2007)

Table S2: Plate rotation parameters

Ang. Vel.	Plate	Wx (°/My)	±	Wy (°/My)	±	Wz (°/My)	±	ρ_{XY}	ρ_{XZ}	ρ_{YZ}
	INDI	0.300919	0.004586	-0.001561	0.019726	0.398902	0.007040	0.927	0.899	0.962
	EURA	-0.032969	0.002504	-0.134905	0.002111	0.206559	0.004237	0.289	0.585	0.456
	INDI-EURA	0.333888	0.005454	0.133344	0.019968	0.192343	0.008323	0.788	0.775	0.817
Euler Pole	Plate	Lat (°)	±	Long (°)	±	Mag (°/My)	±	ρ_{LtLg}	ρ_{LtMg}	ρ_{LgMg}
	INDI	52.970	0.217	-0.297	3.760	0.499677	0.008133	0.406	0.412	0.972
	EURA	56.086	0.869	-103.733	0.964	0.248904	0.002994	0.487	0.701	0.459
	INDI-EURA	28.146	0.560	21.770	2.709	0.407747	0.013893	0.154	0.304	0.933

Table S3: Dislocation model parameters

Fault	End Point 1*	End Point 2*	Width† km	Depth‡ km	Dip	Estimated Slip Rate Strike-slip(mm/yr)	Dip-slip (mm/yr)
1	28.281 °N 79.014 °E	27.118 °N 89.586 °E	999.1	24.1	−10 °	1.2± 0.6	-16.3 ± 0.6
2	26.935 °N 90.004 °E	28.464 °N 99.796 °E	999.0	20.0	−10 °	6.3 ± 0.7	-20.2 ± 0.7
3	25.517 °N 90.064 °E	25.282 °N 93.036 °E	504.1	37.7	0 °	-1.5 ± 0.6	-10.8 ± 0.5

*West and east locations of buried dislocation edge
†Down-dip width
‡Depth to upper edge of rectangular N-dipping dislocation

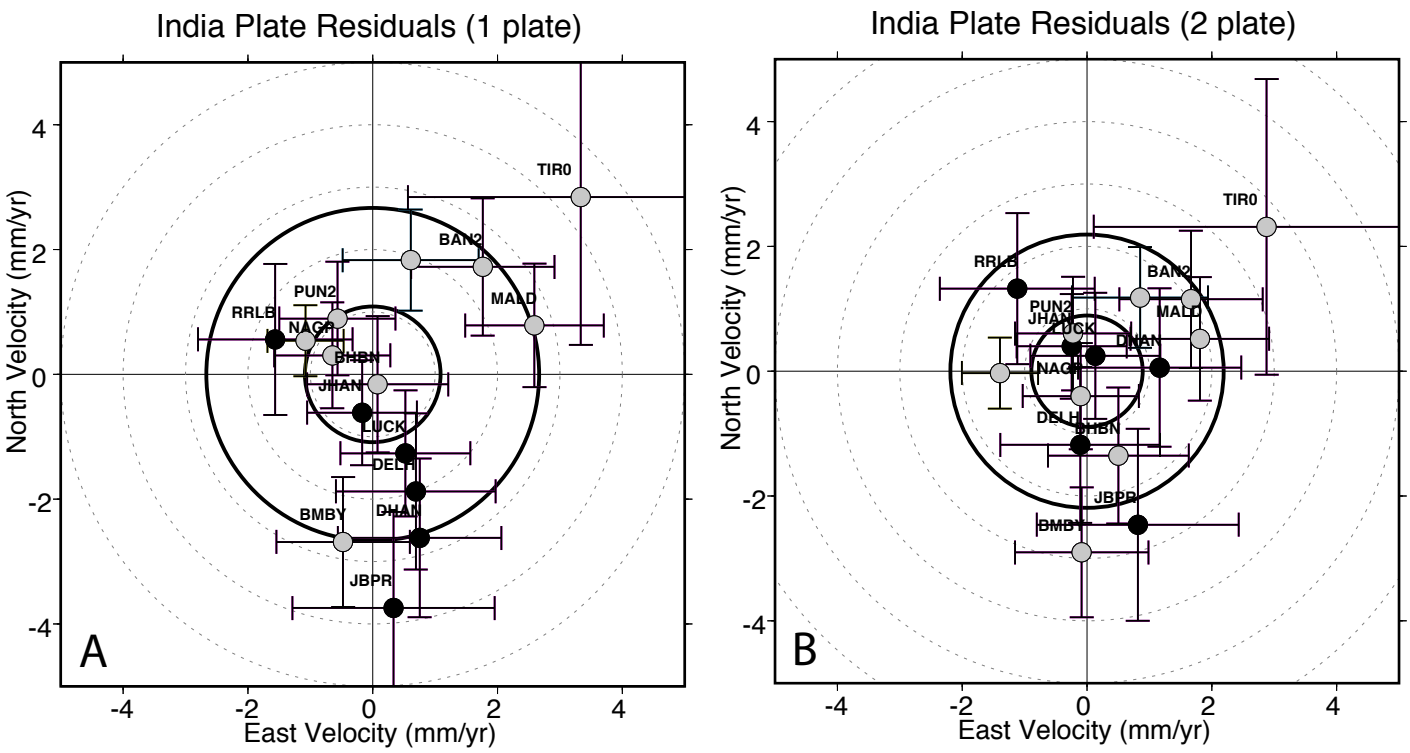
India Plate Residuals (1 plate)
North Velocity (mm/yr)
East Velocity (mm/yr)
TIR0
BAN2
MALD
PUN2
RRLB
NAGP
BHBN
JHAN
LUCK
DELH
DHAN
BMBY
JBPR
A
India Plate Residuals (2 plate)
North Velocity (mm/yr)
East Velocity (mm/yr)
TIR0
RRLB
BAN2
PUN2
JHAN
LUCK
MALD
DHAN
NAGP
DELH
BHBN
JBPR
BMBY
B